Human Cell (2022) 35:1375–1390
https://doi.org/10.1007/s13577-022-00732-2

RESEARCH ARTICLE

Exosomes from human adipose-derived mesenchymal stromal/stem cells accelerate angiogenesis in wound healing: implication of the EGR-1/lncRNA-SENCR/DKC1/VEGF-A axis

Yang Sun[1] · Yikun Ju[1] · Bairong Fang[1]

Received: 10 December 2021 / Accepted: 30 May 2022 / Published online: 25 June 2022

Abstract

Exosomes (Exos) extracted from human adipose mesenchymal stromal/stem cells (hAD-MSCs) have been reported as therapeutic tools for tissue repair, but how they regulate angiogenesis of endothelial cells remains unknown. In this study, hAD-MSCs were isolated, and early growth response factor-1, Smooth muscle and endothelial cell enriched migration/differentiation-associated long-noncoding RNA (lncRNA-SENCR), and vascular endothelial growth factor-A (VEGF-A) overexpression or knockdown was achieved. Exos extracted from hAD-MSCs (hADSC-Exos) were co-cultured with human umbilical vein endothelial cells (HUVECs) to detect the effects of EGR-1, lncRNA-SENCR, and VEGF-A on angiogenesis and the relationships between EGR-1, lncRNA-SENCR, Dyskerin pseudouridine synthase 1 (DKC1), and VEGF-A. An in vivo experiment verified the effect of hADSC-Exos on the wound healing process. hADSC-Exos substantially promoted the proliferation, migration, and angiogenesis of HUVECs, which could be reversed by short-hairpin RNA SENCR (shSENCR) transfection. hADSC-Exos had elevated expression of EGR-1, which bound to the lncRNA-SENCR promoter. The suppressive effect of Exo-shEGR1 on HUVECs was counteracted by SENCR overexpression. LncRNA-SENCR was shown to interact with DKC1. Overexpression of DKC1 or lncRNA-SENCR maintained stable VEGF-A expression. Overexpression of VEGF-A reversed the suppressive effect of shSENCR on HUVECs. Consistent results were obtained in mice in vivo. Overall, hADSC-Exo EGR-1 upregulates lncRNA-SENCR expression to activate the DKC1/VEGF-A axis, facilitating the wound-healing process by increasing angiogenesis.

Keywords Adipose tissue-derived stromal cells · Exosome · EGR-1 · LncRNA-SENCR · DKC1/VEGF-A · Wound healing

Introduction

Patients with diabetes mellitus and chronic peripheral vascular disease ulcers often suffer from non-healing wounds, which unfortunately increase the risk of limb amputation and eventually result in increased medical burden in modern societies [1, 2]. The wound healing process requires the coordination of dermal and epidermal cells, fibroblasts, and endothelial cells [3, 4] within the surrounding extracellular matrix (ECM) [5] to produce three stages: inflammation, proliferation, and matrix remodeling. The dynamic interaction of these cells is regulated by various growth factors such as fibroblast growth factor, platelet-derived growth factor, transforming growth factor, and vascular endothelial growth factor (VEGF) [6]. Uncontrolled wound healing is often associated with a limited ability to generate the microvasculature through angiogenesis [7]. Angiogenesis refers to the process by which new blood vessels are formed from existing vessels, and it has been proven to be related with embryonic development, wound healing, and tumorigenesis to a certain extent [8]. Currently, the therapeutic approach for promoting wound healing includes the delivery of growth factors, gene and stem cell therapies, and mechanical/pressure-based stimulation, among which adipose mesenchymal stromal/stem cells (ADSCs) seem to possess the greatest potential for clinical application, considering their ease of use and regulation of angiogenesis and epithelialization in the wound area [9, 10]. However, how ADCSs

Yang Sun and Yikun Ju have contributed equally to this research.

✉ Bairong Fang
fbrfbr2004@csu.edu.cn

[1] Department of Plastic and Aesthetic (Burn) Surgery, The Second Xiangya Hospital, Central South University, No. 139, Mid Renmin Road, Furong District, Changsha, Hunan 410011, People's Republic of China

facilitate angiogenesis and neovascularization in wounded tissue remains to be determined.

Exosomes (Exos) are extracellular vesicles with an average diameter of 40–160 nm that are mainly responsible for intercellular communication [11]. Depending on their release site, Exos can carry different constituents, including DNA, micro-RNA (miRNA), lipids, and cytosolic and cell surface proteins [12]. Exos derived from hypoxia-induced ADCSs have been proven to mediate angiogenesis in fat grafting by regulating the VEGF/VEGF-receptor pathway [13] and Exos derived from ADCSs (ADSC-Exos) have been proposed as novel therapeutic tools for soft tissue repair [14]. Although studies have supported the application of ADSC-Exos in wound repair, the mechanism is still far from being fully elucidated [15, 16].

Delayed wound healing can be ascribed to local hypoxic conditions and failure of cells to respond to hypoxia [17], during which the transcriptional expression of early growth response factor-1 (EGR-1) is stimulated [18] to regulate the ECM in the development, homeostasis, and healing processes of many tissues [19]. EGR-1 was reported to regulate scar formation through activation of fibroblasts and secretion of massive ECM [20] and to promote tendon healing under reduced load conditions [21]. As a zinc finger transcription factor, EGR-1 is closely associated with cell proliferation, differentiation, and angiogenesis [22]. However, how EGR-1 regulates the ECM and angiogenesis during the wound healing process remains elusive. However, it has also been reported that overexpression of EGR-1 can inhibit wound healing [18], a controversy that may be explained by the downstream targets of EGR-1 according to specific circumstances.

Considering the relationship between ECM, ADSC-Exos, EGR-1, and wound healing, it is intriguing to explore whether EGR-1 is expressed in ADSC-Exos and to further determine whether and how EGR-1 in ADSC-Exos regulates the wound healing process. In the current study, we found that EGR-1 was highly expressed in human ADSC-Exos (hADSC-Exos). Furthermore, EGR-1 in hADSC-Exos accelerated the wound healing process by enhancing angiogenesis of human umbilical vein endothelial cells (HUVECs), which was related with its regulation of the Smooth muscle and endothelial cell enriched migration/differentiation-associated long-noncoding RNA (lncRNA-SENCR)/Dyskerin pseudouridine synthase 1 (DKC1)/VEGF-A axis.

Materials and methods

Compliance with ethical standards

The experimental design involving human was approved by the ethical committee of the Second Xiangya Hospital (approval no. 2019224) and conformed to the Declaration of Helsinki. Human adipose tissues were collected after each enrolled patient provided written informed consent. Animal experiments complied with the regulations and codes of practice for the management of laboratory animals and were reviewed and approved by the ethical committee of the Second Xiangya Hospital (approval no. 2020256).

Isolation and identification of hADSCs

Human adipose tissue was collected from female patients admitted to the plastic surgery department of the Second Xiangya Hospital for liposuction in the abdominal region. The enrolled patients were aged between 20 and 40 years. After obtaining written informed consent, human adipose tissues were collected and washed twice in D-Hanks buffer solution containing penicillin and streptomycin. After centrifugation at 1000×*g* for 3 min, the adipose tissues in the upper layer were transferred into a new 50 mL centrifuge tube using a pipette and then digested with 0.2% collagenase P (Life Technologies Corporation) at 37 °C for 30 min. Then, a certain amount of D-Hanks' solution was added, and the adipose tissues were filtered through a 100 μm cell strainer. The filtered tissues were centrifuged at 1500×*g* for 10 min, and the supernatant was removed. Cells were resuspended in D-Hanks' solution and washed in phosphate-buffered saline (PBS) once, before resuspension in Dulbecco's modified Eagle's medium (DMEM) at 37 °C with 5% CO_2, containing 10% fetal bovine serum (FBS) and 1% antibiotics. After 48 h, cells that were not attached to the culture tube walls were removed. The culture medium was refreshed every 2–3 days. Once the cell confluence reached 80%, the cells were ready for cell passage or cell cryopreservation.

The expression of ADSC biomarkers, including CD90, CD105, CD34, and CD45, was measured using flow cytometry. To assess adipogenesis or osteogenesis, the ADSCs of the 3rd–5th generation were seeded in six well plates at the density of $2 \times 10^4/cm^2$. Once the cell confluency reached 90%, the cells were treated with adipogenesis- or osteogenesis-inducing culture medium (Cyagen) according to the manufacturer's instructions. Mineral and lipid contents were assessed by alizarin red S staining and oil red staining (Sigma Aldrich).

Cell culture

HUVECs were purchased from the Chinese Academy of Sciences (Shanghai, China) and cultured in RPMI 1640 culture

medium (Gibco, NY, USA). The culture medium contained 10% FBS and 1% mycillin, and the cells were cultured at 37 °C with 5% CO_2 and 95% humidity.

Extraction and identification of Exos

hADSCs transfected with short-hairpin RNA (shRNA) targeting EGR-1 (shEGR1) or its negative control (shNC) and untransfected hADSCs were cultured in FBS-free DMEM/F-12 for 36–48 h. The conditioned culture medium was collected and centrifuged at 300×*g* for 10 min to remove cells, and further centrifuged at 2000×*g* for 20 min to remove cell debris. The supernatant was collected and centrifuged at 10,000×*g* for 60 min to remove apoptotic bodies and cell debris, filtered through a 0.22 μm strainer, and subjected to ultracentrifugation (Beckman Optima™ XPN, 45Ti) at 100,000×*g* and 4 °C for 16 h to precipitate the Exos. The Exos were washed with PBS and resuspended in PBS before preservation at − 80 °C. The collected Exos were renamed Exo-shEGR1, Exo-shNC, or hADSC-Exo.

Transmission electron microscopy (TEM; HITACHI H-7000FA, Japan) was used to identify the morphology of Exos. ADSC-Exos (20 μL) were transferred into a formvar/carbon-coated grid and fixed using 2% glutaraldehyde. After staining with 2% phosphotungstic acid, Exos were observed using TEM. The particle distribution and concentration of Exos were analyzed using ZetaView PMX 110 (Particle Metrix, Meerbusch, Germany) and ZetaView software version 8.04.02 through nanoparticle tracking analysis (NTA). The expression levels of the Exos biomarkers CD63, CD9, TSG101, HSP70, calnexin, and GM130 were measured by western blotting.

Cell transfection

Human amnion-derived mesenchymal stem cells (hAD-MSCs) or HUVECs were transfected with sh-EGR1 (100 nM), shRNA targeting lncRNA-SENCR (sh-SENCR, 100 nM), or its negative control (sh-NC). Transfected cells with stable expression were screened using puromycin. To achieve lncRNA-SENCR and VEGF-A overexpression, we transfected the lncRNA-SENCR and VEGF-A targeted pcDNA3.1 vector or pcDNA3.1, respectively, (negative control) into HUVECs.

Experimental groups were classified into control group (HUVECs without any treatment), Exo-shNC group (Exos isolated from hAD-MSCs transfected with sh-NC), Exo-shEGR1 group (Exos isolated from hAD-MSCs transfected with shEGR1), shSENCR group (HUVECs transfected with shSENCR), hADSC-Exo + shNC group (HUVECs co-treated by hAD-MSCs-derived Exos and sh-NC transfection), hADSC-Exo + shSENCR group (HUVECs co-treated by hAD-MSCs-derived Exos and shSENCR transfection), Exo-shEGR1 + vector group (HUVECs co-treated by Exo-shEGR1 and negative control for overexpression lentivirus), Exo-shEGR1 + SENCR group (HUVECs co-treated by Exo-shEGR1 and SENCR overexpression), shSENCR + vector group (HUVECs co-treated by shSENCR and negative control for overexpression lentivirus), and shSENCR + VEGF-A group (HUVECs co-treated by shSENCR and VEGF-A overexpression). All plasmids were purchased from GenePharma (Shanghai, China) and transfected into HUVECs using Lipofectamine 2000 (Invitrogen). The transfection efficiency was verified after transfection for 24 h. The shRNA sequences are presented below.

Sh-EGR1:5'-GCGACATCTGTGGAAGAAAGTGGCATACCAAGATCCACTTGCGCTTTCGGACATGACAGCAAC-3'.

Sh-SENCR:5'-GCAGTGTGGAGATATTTCTTCGGCTCTACCGACCTTCAAACTGCAAGTGACAGATCATCT-3'.

Sh-NC:5'-TTCTCCGAACGTGTCACGT-3'.

Western blotting

Cells were washed twice with cold PBS and then treated with lysis buffer (containing 1% protease inhibitor) on ice for 30 min. After centrifugation at 12,000 rpm and 4 °C for 20 min, the supernatant was collected, and the protein concentration was measured using a bicinchoninic acid (BCA) quantitation kit (Vazyme, Nanjing, China). The proteins (30 μg) were separated on a 10% sodium dodecyl sulfate polyacrylamide gel and transferred onto polyvinylidene difluoridemembranes (Millipore, Billerica, MA, USA) for blocking with 5% skimmed milk for 1 h. The proteins were then incubated with rabbit anti-human CD63 (D4I1X, 1:1000; Cell Signaling Technology, Boston, MA, USA), CD9 (D3H4P, 1:1000; Cell Signaling Technology), TSG101 (D1O5S, 1:1000), HSP70 (6B3, 1:1000), calnexin (C5C9, 1:1000), GM130 (D6B1, 1:1000; Cell Signaling Technology), VEGF-A (PA5-85171, 1:1000; Thermo Fisher Scientific), DKC1 (D6N4K, 1:1000), CD31 (#3528, 1:1000), and EGR1 (#4154, 1:1000) overnight at 4 °C, followed by tris buffered saline with Tween (TBST) washing three times, each for 10 min. The proteins were then incubated with horseradish peroxidase (HRP)-labeled goat anti-rat or goat anti-rabbit immunoglobulin G (IgG, 1:5000; Beijing CoWin Biotech Co., Ltd, Beijing, China) at room temperature for 1 h, followed by washing with TBST three times for 10 min

each. Images were visualized and analyzed using a chemiluminescence imaging system (Tanon Science and Technology Co., Ltd., Shanghai, China). Beta-actin (ACTB) was used as an internal control.

Quantitative real-time PCR (qRT-PCR)

The culture medium was removed, the cells were washed twice with PBS, and 1 mL TRIzol reagent (Life Technologies Corporation) was added using an enzyme-free pipette. Cells were then maintained for 5 min before 200 µL chloroform was added, shaken for 15 s, and mixed for 5 min before centrifugation at 12,000×*g* and 4 °C for 15 min. The solution in the upper layer was transferred into a new enzyme-free Eppendorf tube; an equal volume of isopropanol was added and the mixture was incubated for 10 min before centrifugation at 4 °C and 12,000×*g* for 15 min. The supernatant was removed, the RNA sediment was washed twice with 1 mL of pre-cooled 75% ethyl alcohol, and the resulting supernatant was also removed. Then, enzyme-free diethyl pyrocarbonate (DEPC) was used to dissolve the RNA sediments. The concentration and purity of RNA were determined using an automatic microplate reader (BioTek Synergy2). The RNA was then reverse-transcribed into cDNA using a PCD amplifier, and qRT-PCR was performed using a PCR analyzer (Bio-Rad, CFX Connect). GAPDH was used as the internal control. The conditions were as follows: pre-denaturation at 95 °C for 10 min, 40 cycles of denaturation at 95 °C for 10 s, annealing at 60 °C for 20 s, and extension at 72 °C for 34 s. Data were analyzed using the $2^{-\Delta\Delta Ct}$ method [23]: $\Delta\Delta Ct = [Ct_{(target\ gene)} - Ct_{(internal\ gene)}]_{experimental\ group} - [Ct_{(target\ gene)} - Ct_{(internal\ gene)}]_{control\ group}$. The primer sequences used are listed in (Table 1).

Table 1 The primer sequences for reverse transcription polymerase chain reaction

Name of primer	Sequences
EGR1-F	5′-TGACCGCAGAGTCTTTTCCT-3′
EGR1-R	5′-TGGGTTGGTCATGCTCACTA-3′
LncRNA-SENCR-F	5′-CAGCCAGAAAGGACTCCAACTCC-3′
LncRNA-SENCR-R	5′-GGAG GCAGCTGGTGCTGAAAG-3′
VEGF-A-F	5′-GAGAACGTCACTATGCAGATC-3′
VEGF-A-R	5′-TTTCTCCGCTCTGAACAAGG-3′
GAPDH-F	5′-GTCGATGGCTAGTCGTAGCATCGAT-3′
GAPDH-R	5′-TGCTAGCTGGCATGCCCGATCGATC-3′

F forward, *R* reverse

Uptake of ADSC-Exos by HUVECs

ADSC-Exos (80 µg/mL, 100 µL) were resuspended in 1 mL PBS and then incubated with 4 µL PKH26 fluorochrome at 37 °C for 20 min before centrifugation at 4 °C and 100,000×*g* for 70 min. After removing the supernatant, the ADSC-Exos were washed with PBS and resuspended in 100 µL PBS. HUVECs were resuspended in serum-free culture medium and incubated at 37 °C with 5% CO_2. When the cells showed adherence to the culture tube wall, PKH26-labeled ADSC-Exos were added and incubated for 12 h. HUVECs were then washed twice with PBS and fixed with 4% paraformaldehyde for 4′,6-diamidino-2-phenylindole staining. The uptake of ADSC-Exos was observed using a confocal fluorescence microscope, under which PKH26-labeled ADSC-Exos presented red fluorescence.

Cell counting kit-8 (CCK-8) assay

HUVECs were seeded into 96-well plates (five wells per group) at a density of 1×10^3 cells. Absorbance was determined at the wavelength of 450 nm on days 1, 2, 3, 4, and 5. Cell viability was determined using a CCK-8 kit (Dojindo Molecular Technologies, Kumamoto, Japan). The absorbance of each well was measured using a microplate reader (BioTek).

Wound healing assay

HUVECs were seeded into 96-well plates (three wells per group), and once cell confluency reached 100%, a scratch was made using a 200 µL pipette tip. The cells were then cultured in DMEM containing extracellular vesicles (20, 40, or 80 µg/ml) or PBS (control) for another 24 h. The wound was observed under a phase-contrast microscope at 0 and 24 h. Image-Pro Plus 6 (Media Cybernetics, Inc., Bethesda, MD, USA) was used to observe cell migration. Each experiment was performed at least three times.

Tube formation assay

Matrigel (BD Biosciences, San Jose, CA, USA) was added to a 96-well culture plate, in which HUVECs treated with extracellular vesicles (20, 40, or 80 µg/ml) or PBS (control) for 24 h were seeded for further culture for 6 h. The tube

formation ability of the cells was assessed using a phase-contrast microscope. The tube length was measured using Image-Pro Plus 6, and each experiment was performed at least three times.

Chromatin immunoprecipitation (ChIP) assay

Once HUVECs density reached 80%, cells were collected for PBS washing and resuspended in 1% formaldehyde for 10 min. The resuspended cells were then mixed with 0.125 M glycine solution for 5 min before the crosslinking was terminated. After centrifugation at 4 °C and 300×*g* for 5 min, the sediments were collected for resuspension with cell lysis (1×10^7 cells and 1 mL cell lysate) on ice for 10 min. HUVECs were subjected to ultrasonication and then centrifuged at 4 °C and 12,000×*g* for 10 min, and the supernatant was collected. The crosslinked chromatin at 5–10 μg (100 μL supernatant containing chromatin) was diluted with 400 μL ChIP buffer containing protease inhibitor and then incubated with 10 μL (2 μg) EGR-1 antibody at 4 °C overnight. Further incubation with 30 μL Protein G Magnetic Beads at 4 °C for 2 h enabled full interaction of the antibody with the beads. The Eppendorf tube was placed on a magnetic grate for 30 s, and once the solution was clear, the supernatant was removed and the beads were washed with pre-cooled 0.1 × ChIP buffer three times. The beads were then added to 150 μL ChIP eluting buffer and incubated at 65 °C for 30 min. Chromatin was eluted from antibody/Protein G Magnetic Beads through vortexing (1200 rpm), and the eluted supernatant was incubated with 6 μL 5 M NaCl and 2 μL Proteinase K at 65 °C for 2 h before the chromatin was collected for DNA purification. DNA was quantified by PCR.

Dual-luciferase reporter gene assay

The binding sites of the lncRNA-SENCR promoter with EGR-1 were predicted using the JASPAR database (https://jaspar.genereg.net) and cloned into the luciferase pGL3 reporter vector (Promega, Madison, WI, USA) to establish the promoter-luciferase reporter plasmid. The plasmid was then co-transfected with pcDNA3.1–3*Flag or pcDNA3.1–3*Flag-EGR1 into HUVECs and 48 h later, the luciferase activity was measured using a kit (Promega) to verify the effect of EGR-1 on the lncRNA-SENCR promoter.

RNA pull-down assay

A Pierce™ Magnetic RNA-Protein Pull-Down kit (Thermo Fisher Scientific) was used for RNA pull-down. In vitro transcription was performed for lncRNA-SENCR, which was then labeled with the Pierce™ RNA 3′ End Desthiobiotinylation kit (Thermo Fisher Scientific). The HUVECs lysate (200 μg) was incubated with 50 pmol of purified and biotinylated transcripts for 1 h under rotation at 4 °C. The complexes formed were isolated using streptomycin magnetic beads and then used for western blotting.

RNA immunoprecipitation (RIP) assay

Cells were washed in pre-cooled PBS twice and then added with certain volume of lysis for 5 min at ice for centrifugation at 13,000×*g* for 20 min. The supernatant was collected and protein concentration was determined using the BCA measurement method. The cells were then incubated with magnetic beads coated with human anti-DKC1 (#sc-373956; Santa Cruz Biotechnology Inc., Dallas, TX, USA) or anti-IgG (Merck Millipore, Burlington, MA, USA) at 4 °C overnight, followed by purification with protease K. The expression levels of lncRNA-SENCR and VEGF-A were determined by qRT-PCR.

Detection of protein half-life

HUVECs overexpressing DKC1 or lncRNA-SENCR were cultured in vitro. After cell transfection for 36–48 h, cells from each group were added to complete culture medium, to which 100 μg/mL cycloheximide (CHX) was added for 0, 1, 2, 4, 6, and 8 h. After each of these periods, the cells were collected and protein expression was measured by western blotting.

Mouse wound healing assay

Forty-eight healthy male C57BL/6 J mice (5 weeks old; weight, 20.88 ± 1.94 g) were purchased from Hunan SJA Laboratory Animal Co., Ltd. and housed in cages under a 12:12-h light:dark photoperiod with constant temperature and humidity. Mice were anesthetized with pentobarbital sodium (50 mg/kg; #57-33-0; Shanghai Beizhuo Biotechnology Co., Ltd., China) through intraperitoneal injection. The fur on the back was shaved and the remaining fur was removed using a depilatory. A wound was created on the back using an unsterile puncher (diameter, 10 mm). hADSC-Exo, Exo-shNC, or Exo-shEGR1 was injected into the skin around the wound, and the wound was disinfected using 0.5% iodine daily. Wound healing was monitored and the wound healing rate was calculated: wound

healing rate = (initial wound area − current wound area)/initial wound area × 100%. The tissues of and around the wound on days 0, 3, 7, and 13 were collected and fixed using 10% paraformaldehyde for embedding and hematoxylin and eosin (H&E) staining.

H&E staining

The skin tissues were cut into 5 μm slices and then dewaxed in xylene twice (15 min each time) before washing with absolute ethyl alcohol twice (5 min each time). The slices were then hydrated in a graded ethanol solution series (95, 80, and 70%; each for 5 min), and washed again before hematoxylin staining for 10 min. After washing in running water for 5 min, the slices were treated with 1% hydrochloric acid alcohol and stained with 1% eosin for 30 s after another round of washing. Excess eosin was removed by washing, and the slices were then hydrated in an ethyl alcohol series (95, 95, 100, and 100%; each for 1 min) before being made transparent with xylene solution twice, each for 3 min. Tissue staining was observed under a light microscope.

Immunohistochemistry

The skin tissues were cut into 5 μm slices and dewaxed with xylene I and xylene II for 15 min each before washing with absolute ethyl alcohol twice for 5 min each. The slices were then hydrated in a graded ethanol solution series (95, 80, and 70%; 5 min each), and then washed again. A sodium citrate buffer was used for high-pressure antigen retrieval at 115 °C for 5 min. The slices were treated with 3% hydrogen peroxide solution at room temperature for 10 min to remove endogenous peroxidase, and then blocked with 5% bovine serum albumin at room temperature for 1 h before further incubation with primary antibodies against CD31 (#3528, 1:1000; Cell Signaling Technology) or VEGF-A (PA5-85171, 1:1000; Thermo Fisher Scientific) overnight at 4 °C and with HRP-labeled secondary antibody for 1 h at room temperature. Diaminobenzidine was used for color development, and cell nuclei were stained with hematoxylin, after which the slices were hydrated, made transparent, and sealed for observation and photography under a light microscope.

Statistical analysis

All data were analyzed using SPSS 17.0. Measurement data are expressed as mean ± standard deviation. Comparisons among groups were performed via one-way analysis of variance using the least significant difference test to verify data compliance with homogeneity of variance; in other cases, the Games–Howell analysis was used. Statistical significance was considered at $p < 0.05$.

Results

Identification and effect of hADSC-Exo on the proliferation, migration, and angiogenesis of endothelial cells

hADSCs were isolated from human adipose tissue and the expression of surface antigens was measured. The results of flow cytometry showed that hADSCs had positive expression of CD90 and CD105 but no or low expression of CD34 or CD45 (Supplementary Fig. 1A). The observation of hADSCs showed that the cells were fibroblast-like (Supplementary Fig. 1B). The differentiation ability of hADSCs was also assessed by oil red O and alizarin red S staining, which showed that hADSCs were capable of differentiating into lipoblasts (Supplementary Fig. 1C) and osteoblasts (Supplementary Fig. 1D). Therefore, the characteristics of the isolated hADSCs were consistent with those of MSCs.

hADSC-Exos were also observed by TEM. The hADSC-Exos presented double-membrane structure and were mainly circular, oval, or saucer-shaped (Fig. 1A). The diameter of hADSC-Exos was 80.0 ± 1.9 nm, on average. The average and highest diameters were consistent with those of the Exos. Western blotting detected the expression of CD63, CD9, TSG101, and HSP70, but no expression levels of GM130 or calnexin were found in hADSC-Exos (Fig. 1B). These results indicated that hADSC-Exos were successfully isolated.

hADSC-Exos at 20, 40, or 80 μg/mL were used to treat HUVECs, and the results showed that hADSC-Exos treatment for 3 days induced the proliferation of HUVECs in a dose-dependent manner (Fig. 1C). The cell scratch and tube formation assays showed that co-culture of hADSC-Exos with HUVECs increased the migration and angiogenesis abilities of the latter (Fig. 1D, E). To verify whether hADSC-Exos could enter HUVECs to induce cell migration, proliferation, and angiogenesis, we labeled hADSC-Exos with PKH26. The results showed that hADSC-Exos were taken up by HUVECs and distributed around the cell nucleus (Fig. 1F). Taken together, these results indicate hADSC-Exos enter HUVECs to enhance cell proliferation, migration, and angiogenesis.

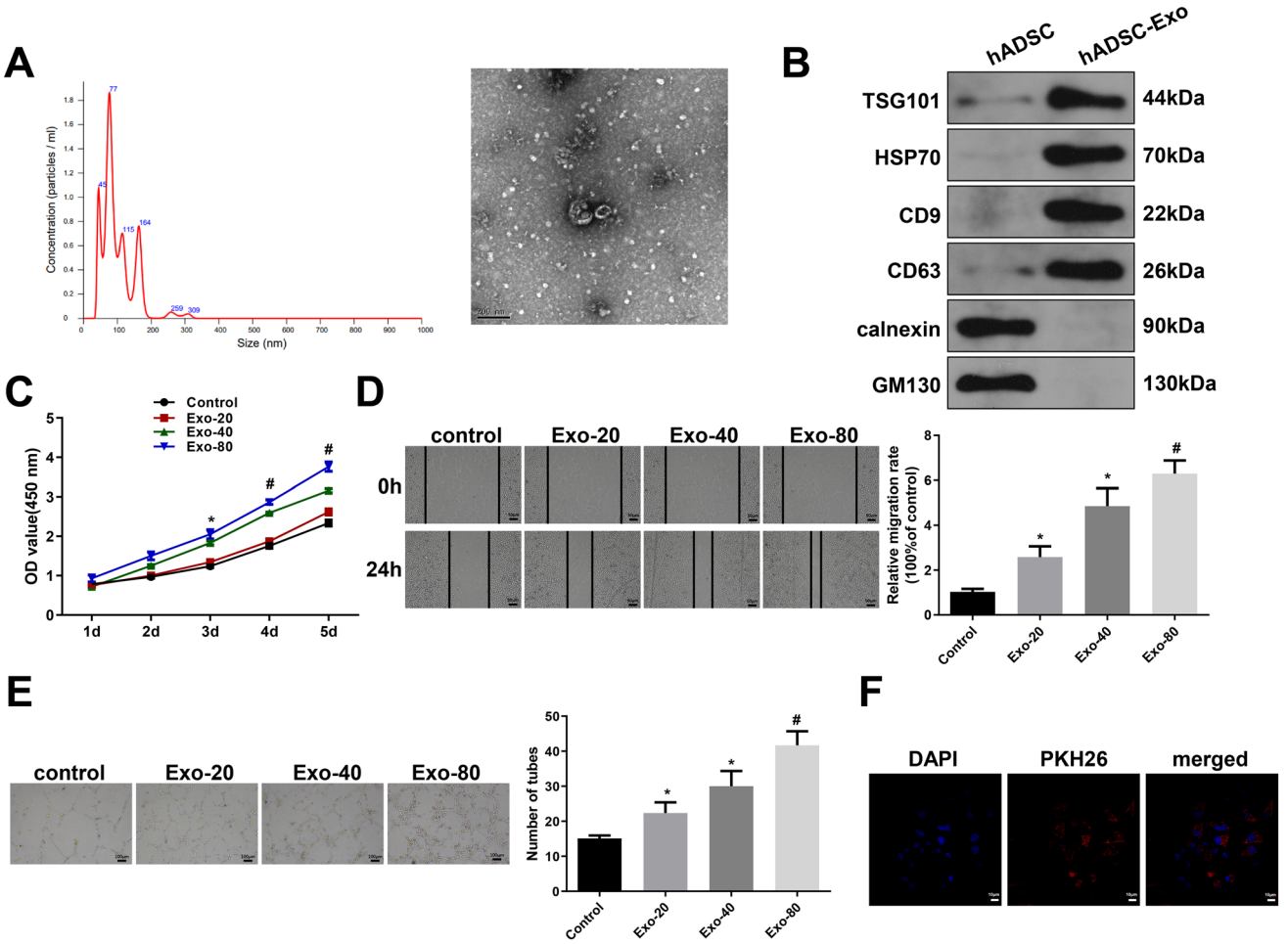

Fig. 1 hADSC-Exo promotes the proliferation, migration and angiogenesis of endothelial cells. **A** TEM was used to observe the structure of hADSC-Exo and Nanoparticle Tracking Analysis was used to measure the diameter of hADSC-Exo; **B** The biomarkers of exos in hADSC-Exo were measured by western blot; hADSC-Exo was co-cultured with HUVECs, **C** CCK-8 was used to detect the proliferation of hADSC-Exo; (D) cell scratch assay was used to detect the migration of HUVECs; **E** tube formation assay was used to assess the angiogenesis ability of HUVECs; **F** PKH26 staining to verify whether hADSC-Exo can move into HUVECs; *compared with control group, $p < 0.05$; **compared with control group, $p < 0.01$. HUVECs, human umbilical vein endothelial cells; Exo, exosome; hADSC-Exo, exosomes derived from human adipose mesenchymal stromal/stem cells. All experiments were conducted for three times and triplicate wells were set for each experiment

Knockdown of EGR-1 in hADSC-Exos regulates the proliferation, migration, and angiogenesis of endothelial cells

To explore how hADSC-Exos regulate the biological functions of HUVECs, we measured the expression of EGR-1 in HUVECs after co-culture with hADSC-Exos. qRT-PCR and western blotting demonstrated that the mRNA and protein expression of EGR-1 increased with increasing concentrations of hADSC-Exos (Fig. 2A, B). EGR-1 shRNA was transfected into hADSCs to knockdown the expression of EGR-1, from which Exo-shEGR1 was isolated. Compared with the Exo-shNC group, the mRNA and protein expression of EGR-1 was reduced in the Exo-shEGR1 group (Fig. 2C, D). Exo-shEGR1 was then co-cultured with HUVECs, and measurements showed that Exo-shEGR1 substantially suppressed the proliferation (Fig. 2E), migration (Fig. 2F), and angiogenesis (Fig. 2G) of HUVECs compared with those co-cultured with Exo-shNC. These results suggest that EGR-1 in hADSC-Exos enhances the proliferation, migration, and angiogenesis of HUVECs.

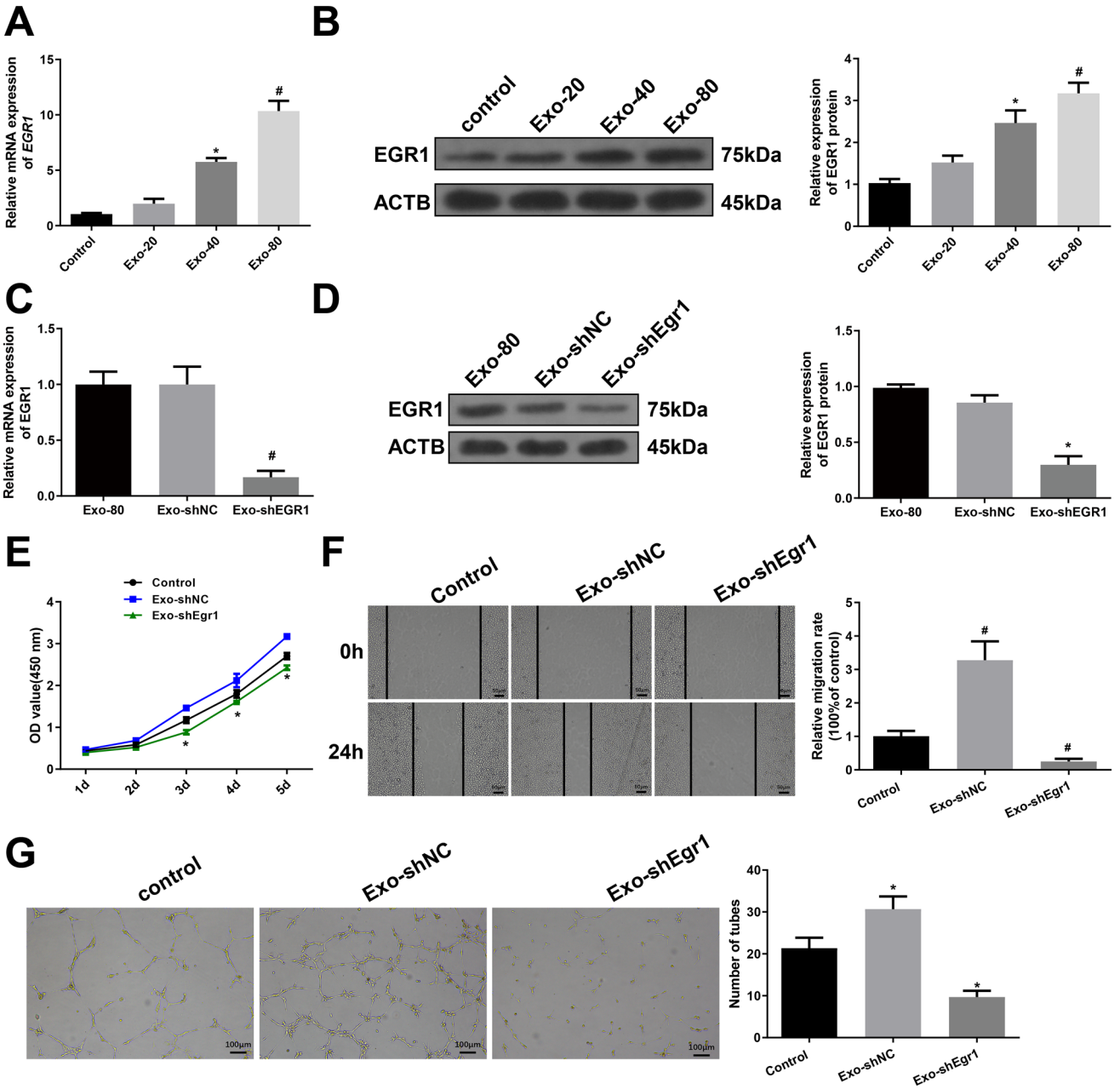

Fig. 2 Suppression on EGR1 in hADSC-Exo can inhibit the proliferation, migration and angiogenesis of HUVECs. **A** qPCR detected the expression of *EGR1* mRNA in hADSC-Exo *compared with control group, $p<0.05$; **compared with control group, $p<0.01$; **B** western blot measured the EGR1 protein expression in hADSC-Exo, *compared with control group, $p<0.05$; **compared with control group, $p<0.01$; after HUVECs were co-cultured with Exo-shEGR1, **C** qPCR was used to detect the *EGR1* mRNA expression, #, compared with Exo-shNC group, $p<0.05$; **D** western blot measured the EGR1 protein expression in HUVECs, #, compared with Exo-shNC group, $p<0.05$; **E** CCK-8 was applied to detect the effect of Exo-shEGR1 on proliferation of HUVECs, *Exo-shNC group compared with control group, $p<0.05$; #, Exo-shEGR1 group compared with Exo-shNC group, $p<0.05$; **F** cell scratch assay was utilized to assess the effect of Exo-shEGR1 on migration of HUVECs, *Exo-shNC group compared with control group, $p<0.05$; #, Exo-shEGR1 group compared with Exo-shNC group, $p<0.05$; **G** tube formation assay was used to assess the effect of Exo-shEGR1 on angiogenesis of HUVECs, *Exo-shNC group compared with control group, $p<0.05$; #, Exo-shEGR1 group compared with Exo-shNC group, $p<0.05$; hADSC-Exo, exosomes extracted from human adipose mesenchymal stromal/stem cells; HUVECs, human umbilical vein endothelial cells. All experiments were conducted for three times and triplicate wells were set for each experiment

EGR-1 binds the lncRNA-SENCR promoter to increase proliferation, migration, and angiogenesis of HUVECs

The JASPAR database revealed that EGR-1 can bind to the promoter of lncRNA-SENCR (Supplementary Fig. 3A). After HUVECs were co-cultured with Exo-shEGR1, the qRT-PCR results allowed comparing the expression of lncRNA-SENCR in HUVECs of the Exo-shEGR1 group with those in the Exo-shNC group (Fig. 3A). ChIP analysis of the interaction between EGR-1 and the promoter of lncRNA-SENCR in HUVECs (Fig. 3B) was further verified by a dual-luciferase reporter gene assay (Fig. 3C). To determine the role of lncRNA-SENCR, lncRNA-SENCR knockdown was performed in HUVECs (Fig. 3D). Further measurements showed that inhibition of lncRNA-SENCR expression resulted in suppressed cell proliferation (Supplementary Fig. 2A), migration (Supplementary Fig. 2B), and angiogenesis (Supplementary Fig. 2C) of HUVECs.

Next, we aimed to verify the effect of the interaction between lncRNA-SENCR and EGR-1 in HUVECs. HUVECs were co-cultured with hADSC-Exo or Exo-shEGR1 for 48 h before transfection with shSENCR or SENCR, followed by treatment with Exo-shEGR1. The measurement of HUVECs showed that knockdown of lncRNA-SENCR could reverse the effect of hADSC-Exo on HUVECs proliferation (Fig. 3E), migration (Fig. 3G), and angiogenesis ability (Fig. 3I), which also restored the suppressive effect of Exo-shEGR1 on the proliferation (Fig. 3F), migration (Fig. 3H), and angiogenesis ability (Fig. 3J) of HUVECs. These results showed that EGR-1 can bind to the lncRNA-SENCR promoter to induce the expression of lncRNA-SENCR and, therefore, enhance the proliferation, migration, and angiogenesis ability of HUVECs.

LncRNA-SENCR can recruit DKC1 to enhance the stability and expression of VEGF-A

The starBase database predicted the binding sites of lncRNA-SENCR with DKC1 (Supplementary Fig. 3B). The RNA pull-down assay demonstrated the binding of lncRNA-SENCR with DKC1, and RIP detected the interaction between lncRNA-SENCR and DKC1. As shown in (Fig. 4A), DKC1 was enriched by lncRNA-SENCR, whereas antisense RNA was not. RIP demonstrated that DKC1 in HUVECs interacted with lncRNA-SENCR (Fig. 4B). These results indicate that lncRNA-SENCR can specifically target DKC1 in HUVECs.

The starBase database also predicted the binding site of DKC1 and VEGF-A (Supplementary Fig. 3C), which was verified by RIP (Fig. 4C), indicating lncRNA-SENCR can bind to DKC1 to regulate VEGF-A expression. Interestingly, compared to the untreated group, HUVECs treated with Exo-shNC showed increased expression of VEGF-A, while the Exo-shEGR1 treatment significantly suppressed VEGF-A expression (Fig. 4D). Knockdown of lncRNA-SENCR also suppressed VEGF-A expression (Fig. 4E). In addition, DKC1 or lncRNA-SENCR overexpression substantially extended the half-life period of HUVECs (Fig. 4F–G).

VEGF-A overexpression can reverse the effect of lncRNA-SENCR knockdown on HUVECs

VEGF-A was overexpressed in HUVECs (Fig. 5A, B). The CCK-8 assay showed that shSENCR suppressed cell proliferation, which was reversed by VEGF-A overexpression (Fig. 5C). The cell scratch assay showed that shSENCR significantly suppressed the migration of HUVECs, while VEGF-A overexpression suppressed the effect of shSENCR on cell migration (Fig. 5D). Similarly, shSENCR suppressed the angiogenesis ability of HUVECs, whereas cell angiogenesis was restored after co-treatment with shSENCR and VEGF-A overexpression plasmids (Fig. 5E). These results showed that the regulatory role of lncRNA-SENCR in the proliferation, migration, and angiogenesis of HUVECs is related to VEGF-A upregulation in HUVECs.

EGR-1 in hADSC-Exos regulates the lncRNA-SENCR/VEGF-A axis to improve wound healing in mouse by increasing cell angiogenesis ability

Wounds were made on the backs of healthy mice, which were then injected with Exo-shNC, Exo-shEGR1, or PBS. Wound healing was observed on days 0, 3, 7, and 13. As shown in (Fig. 6A), no significant differences were observed among the groups on day 3. On days 7 and 13, the wound area in the Exo-shNC group was smaller than that in the other groups ($p < 0.05$), whereas that in the Exo-shEGR1 group was larger than that in the other groups (Fig. 6A). These results showed that hADSC-Exos may carry EGR-1 to promote wound healing in mice. Analysis of the regenerated dermal tissues on day 14 revealed that the granulation tissues in each group were complete and thick (Fig. 6B). New hair follicles were found in the wound area of the

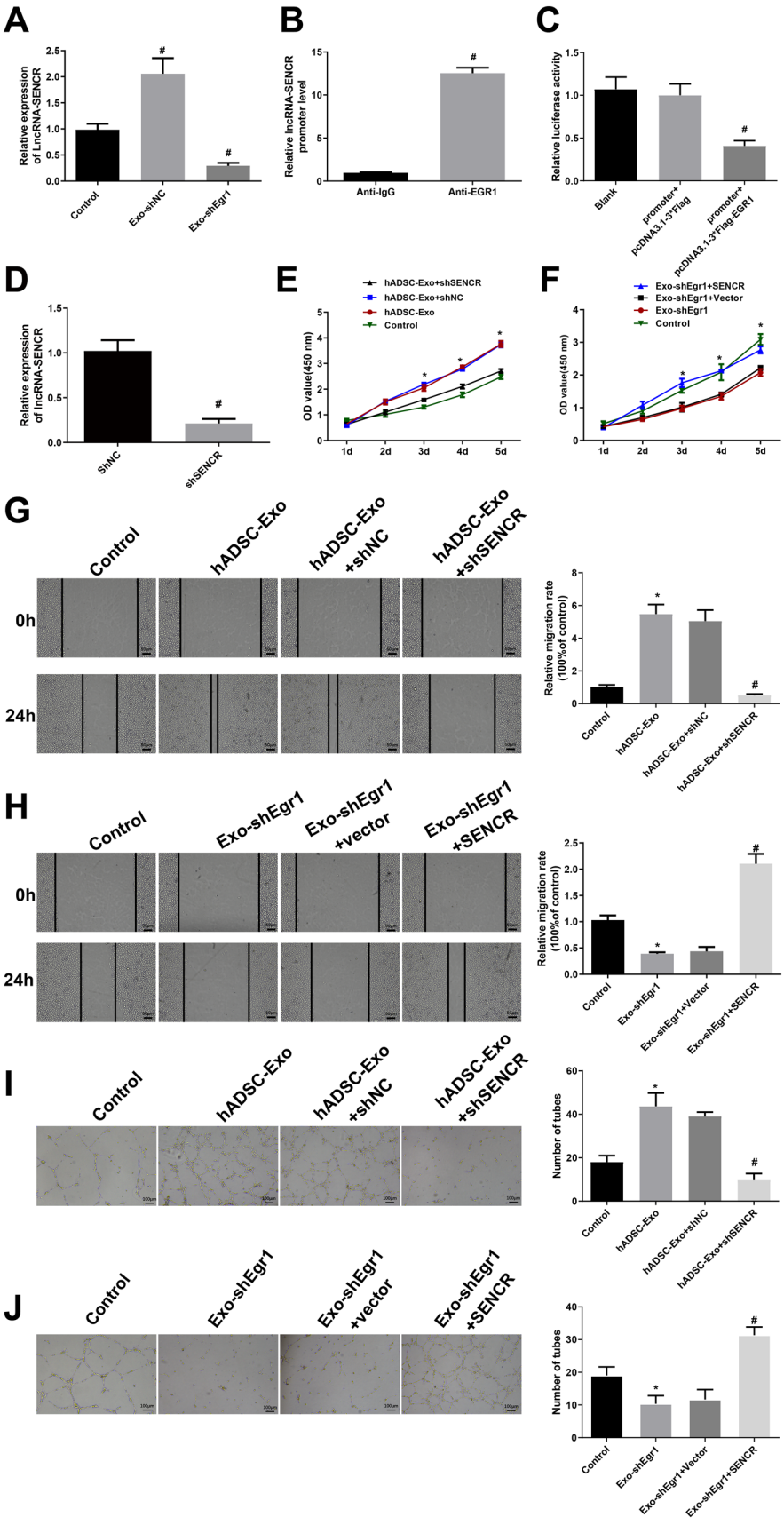
A
Relative expression of LncRNA-SENCR
Control
Exo-shNC
Exo-shEgr1
B
Relative lncRNA-SENCR promoter level
Anti-IgG
Anti-EGR1
C
Relative luciferase activity
Blank
promoter+ pcDNA3.1-3*Flag
promoter+ pcDNA3.1-3*Flag-EGR1
D
Relative expression of lncRNA-SENCR
ShNC
shSENCR
E
hADSC-Exo+shSENCR
hADSC-Exo+shNC
hADSC-Exo
Control
OD value(450 nm)
1d
2d
3d
4d
5d
F
Exo-shEgr1+SENCR
Exo-shEgr1+Vector
Exo-shEgr1
Control
OD value(450 nm)
G
Control
hADSC-Exo
hADSC-Exo +shNC
hADSC-Exo +shSENCR
0h
24h
Relative migration rate (100%of control)
H
Control
Exo-shEgr1
Exo-shEgr1 +vector
Exo-shEgr1 +SENCR
0h
24h
Relative migration rate (100%of control)
I
Control
hADSC-Exo
hADSC-Exo +shNC
hADSC-Exo +shSENCR
Number of tubes
J
Control
Exo-shEgr1
Exo-shEgr1 +vector
Exo-shEgr1 +SENCR
Number of tubes

◂**Fig. 3** EGR1 can bind lncRNA-SENCR promoter to suppress proliferation, migration and angiogenesis ability of endothelial cells. **A** qPCR detected the expression of lncRNA-SENCR in Exo-shEGR1 treated HUVECs, *Exo-shNC group compared with control group, $p < 0.05$; #, Exo-shEGR1 group compared with Exo-shNC group, $p < 0.05$; **B** ChIP verified EGR1 can directly bind lncRNA-SENCR promoter in HUVECs, **compared with Anti-IgG group, $p < 0.01$; **C** dual-luciferase reporter assay confirmed the interaction of EGR1 with lncRNA-SENCR promoter, ** compared with promoter + pcDNA3.1–3*Flag group, $p < 0.01$; **D** qPCR detected the expression of lncRNA-SENCR in HUVECs after lncRNA-SENCR knockdown, *shSENCR group compared with shNC group, $p < 0.05$; #, SENCR overexpression group compared with vector group, $p < 0.05$; **E** CCK-8 assay detected the cell proliferation of HUVECs after co-treatment with hADSC-Exo and shSENCR, *hADSC-Exo group compared with control group, $p < 0.05$; #, hADSC-Exo + shSENCR group compared with hADSC-Exo + shNC group, $p < 0.05$; **F** CCK-8 assay detected the cell proliferation of HUVECs after co-treatment with Exo-shEGR1 and pcDNA3.1-SENCR, *Exo-shEGR1 group compared with control group, $p < 0.05$; #, Exo-shEGR1 + SENCR group compared with Exo-shEGR1 + vector group, $p < 0.05$; **G** cell scratch assay assessed cell migration ability of HUVECs after co-treatment with hADSC-Exo and shSENCR, *hADSC-Exo group compared with control group, $p < 0.05$; #, hADSC-Exo + shSENCR group compared with hADSC-Exo + shNC group, $p < 0.05$; **H** cell scratch assay assessed cell migration ability of HUVECs after co-treatment with Exo-shEGR1 and pcDNA3.1-SENCR *Exo-shEGR1 group compared with control group, $p < 0.05$; #, Exo-shEGR1 + SENCR group compared with Exo-shEGR1 + vector group, $p < 0.05$; **I** tube formation assay measured the angiogenesis of HUVECs after co-treatment with hADSC-Exo with shSENCR, *hADSC-Exo group compared with control group, $p < 0.05$; #, hADSC-Exo + shSENCR group compared with hADSC-Exo + shNC group, $p < 0.05$; **J** tube formation assay measured the angiogenesis of HUVECs after co-treatment with Exo-shEGR1 and pcDNA3.1-SENCR, *Exo-shEGR1 group compared with control group, $p < 0.05$; #, Exo-shEGR1 + SENCR group compared with Exo-shEGR1 + vector group, $p < 0.05$. hADSC-Exo, exosomes extracted from human adipose mesenchymal stromal/stem cells; HUVECs, human umbilical vein endothelial cells. All experiments were conducted for three times and triplicate wells were set for each experiment

Exo-shNC group, in which proliferation of fibroblasts and well-arranged collagen deposition were also observed. No hair follicle or collagen deposition was found in the control group, and substantial inflammatory infiltration was observed in the Exo-shEGR1 group. The expression of EGR-1, VEGF-A, and lncRNA-SENCR in skin tissues was also detected. Compared to the control group, the Exo-shNC group showed elevated expression of EGR-1, VEGF-A, and lncRNA-SENCR, which was different from that observed in the Exo-shEGR1 group (Fig. 6C–F, H). To further ascertain the effect of Exo-shEGR1 on wound healing, we measured the expression of endothelial biomarker CD31. Compared to that in the control group, the CD31 positive area in the Exo-shNC group was increased, while that in the Exo-shEGR1 group was reduced (Fig. 6G). In vivo experiments demonstrated that hADSC-Exos can improve wound healing in mice by regulating the EGR-1/lncRNA-SENCR/VEGF-A axis.

Discussion

Delayed diabetic wound healing is increasingly becoming a social concern. It results from the failure of sufficient blood flow through the improvement of vascular conditions or neoangiogenesis within the tissues [24]. Angiogenesis is essential and required for multiple physiological and pathological processes, including wound healing and tissue repair [25], as nutrients, oxygen, and growth factors can be transported via the new blood vessels to the injured area [26]. In the present study, we found a possible role for EGR-1 in hADSC-Exos concerning the regulation of endothelial cells angiogenesis. We also investigated the possible mechanism, and the results showed that EGR-1 can activate the lncRNA-SENCR/VEGF-A axis to promote angiogenesis and thus improve the wound healing process.

Exos released by MSCs mimic the effects of parental MSCs and can modulate the biological activity of recipient cells by shuttling various contents, including proteins and RNAs [27]. MSC-Exos, as a cell-free therapeutic tool, has been found to promote immune regulation, vascular regeneration, and partaking in disease processes [28, 29]. Among MSCs, ADSCs have been shown to relate with angiogenesis by overexpressing VEGF [30]. Consistent with a previous study, the measurement of cell proliferation and angiogenesis of HUVECs performed here illustrated that hADSC-Exos treatment could improve the proliferation, invasion, migration, and angiogenesis ability of HUVECs. hADSC-Exos were shown to regulate collagen synthesis during the wound healing process, during which type I and type III collagen secretion was increased in the early stage and collagen synthesis was suppressed in the late stage in response to hADSC-Exo regulation, thus contributing to the suppression of scar formation [31]. Although the role of hADSC-Exos in regulating angiogenesis of endothelial cells has been determined, it is also important to locate each possible content within the hADSC-Exos, which may facilitate such regulation. In the present study, we found that ERG-1 expression increased with the concentration of hADSC-Exos, indicating that ERG-1 was carried by hADSC-Exos. Further functional experiments on cell proliferation and angiogenesis of HUVECs showed that ERG-1 in hADSC-Exos can promote cell proliferation and angiogenesis in endothelial cells, which highlights the possible role of ERG-1 in the

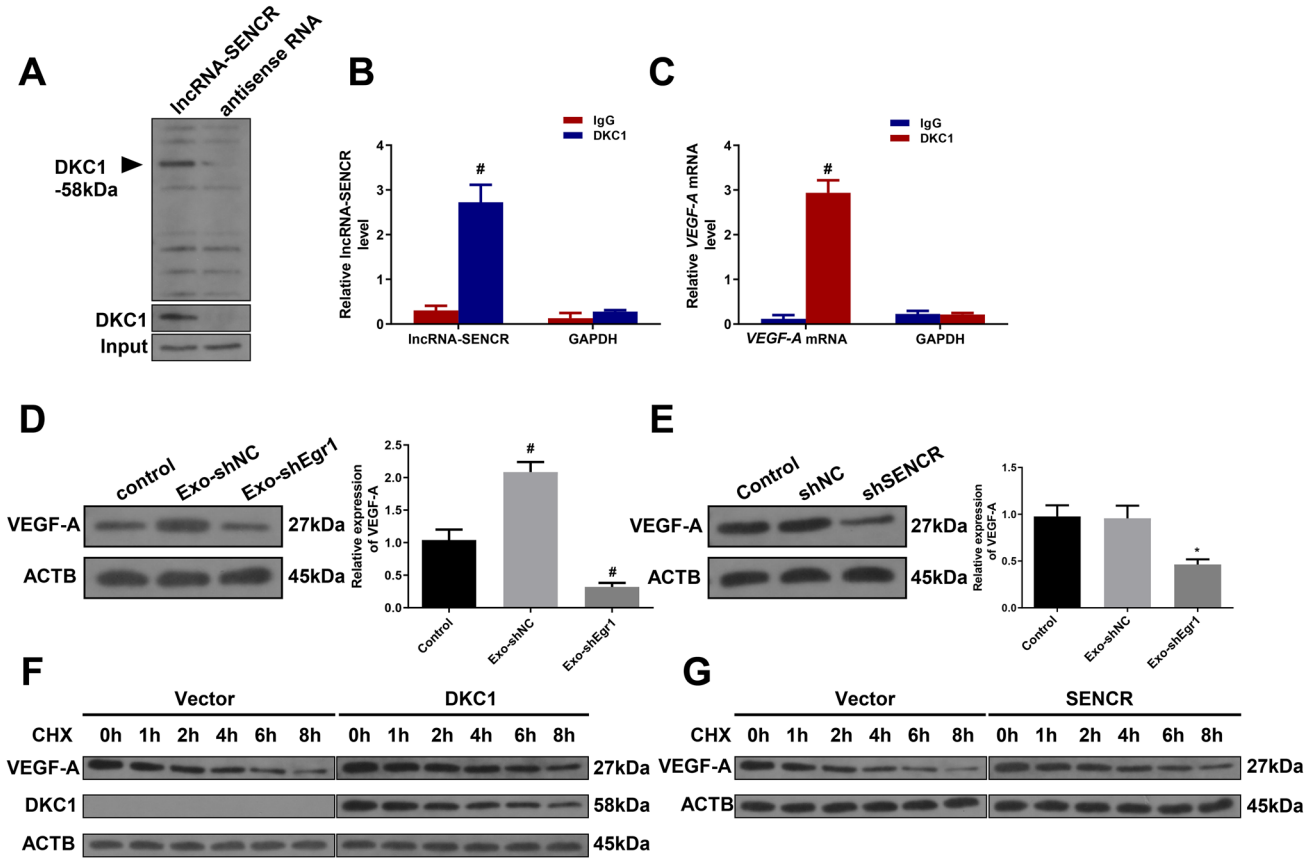

Fig. 4 LncRNA-SENCR can bind DKC1 to increase the expression of VEGF-A. **A** RNA Pull down detected the target relationship between lncRNA-SENCR and DKC1; **B** RIP verified the binding of lncRNA-SENCR with DKC1, **compared with IgG group, $p < 0.01$; **C** RIP identified the binding of DKC1with VEGF-A, **compared with IgG group, $p < 0.01$; **D** western blot measured the expression of VEGF-A in HUVECs after Exo-shEGR1 treatment, *Exo-shNC group compared with control group, $p < 0.05$; #, Exo-shEGR1 group compared with Exo-shNC group, $p < 0.05$; **E** western blot measured the expression of VEGF-A in HUVECs after shSENCR treatment, *compared with Exo-shNC group, $p < 0.05$; **F** protein half-life period measured the effect of DKC1 overexpression on VEGF-A expression; **G** protein half-life period measured the effect of lncRNA-SENCR overexpression on VEGF-A expression. HUVECs, human umbilical vein endothelial cells. All experiments were conducted for three times and triplicate wells were set for each experiment

wound healing process. Although a previous study supported the role of EGF-1 in tissue repair, its repression in adipose tissue-derived MSCs of diabetic patients was reported to promote wound repair activity [18]. The same study also suggested that EGR-1 plays a dual role in wound healing depending on the cellular context, as its biological function can be altered by cellular differentiation. Similar to our study, EGR-1 was also found to be regulated by formononetin through the ERK and p38 MAPK pathways to enhance endothelial repair and wound healing [32]. A possible explanation can be found in an early study that demonstrated that EGR-1 can induce the production of cytokines and growth factors, which is very important for early ECM (collagen) formation [33].

Our study also explored the downstream targets of EGR-1 and showed that EGR-1 can bind to the lncRNA-SENCR promoter, which can further recruit DKC1 to increase the expression of VEGF-A. The DKC1 gene was first discovered because its mutation caused congenital dyskeratosis, whose dysregulation functioned as a tumor suppressor in various cancers [34] but enhanced tumor progression in others [35]. In colorectal cancer cells, DKC1 facilitates angiogenesis and metastasis by increasing hypoxia-inducible factor-1 alpha (HIF-1α) and VEGF-A expression levels [36]. HIF-1α/VEGF-A is a well-known signaling pathway involved in tissue repair and angiogenesis in multiple diseases [37, 38]. VEGF-A is essential for normal endothelial cell function and promotes angiogenesis by enhancing vascular permeability

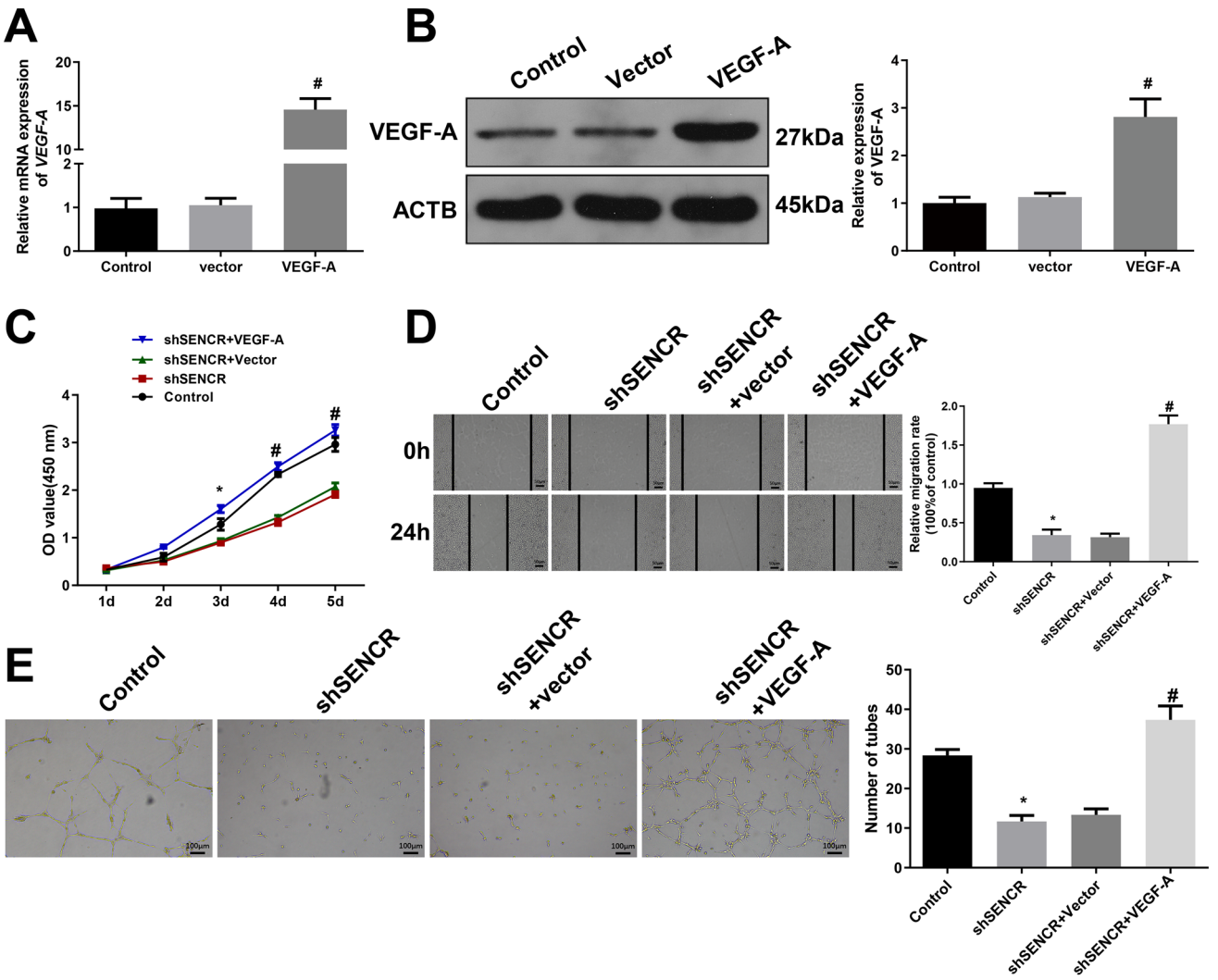

Fig. 5 The regulation of lncRNA-SENCR on proliferation, migration and angiogenesis of HUVECs can be reversed by VEGF-A overexpression. **A** qPCR detected the expression of *VEGF-A* mRNA in HUVECs after VEGF-A overexpression plasmid was transfected, **compared with vector group, $p<0.01$; **B** Western blot measured the expression of VEGF-A in HUVECs after VEGF-A overexpression plasmid was transfected, **compared with vector group, $p<0.01$; **C** CCK-8 detected the cell proliferation of HUVECs after co-treatment by shSENCR with pcDNA3.1-VEGF-A, *shSENCR group compared with control group, $p<0.05$; # shSENCR + vector group compared with shSENCR + VEGF-A group, $p<0.05$; **D** cell scratch assay detected cell migration ability in HUVECs after co-treatment with shSENCR and pcDNA3.1-VEGF-A, *shSENCR group compared with control group, $p<0.05$; #, shSENCR + vector group compared with shSENCR + VEGF-A group, $p<0.05$; **E** tube formation assay assessed angiogenesis of HUVECs after co-treatment with shSENCR and pcDNA3.1-VEGF-A, *shSENCR group compared with control group, $p<0.05$; # shSENCR + vector compared with shSENCR + VEGF-A group, $p<0.05$. HUVECs, human umbilical vein endothelial cells. All experiments were conducted for three times and triplicate wells were set for each experiment

and fibrinogen [39]. Considering its role in angiogenesis, growth factor treatment has been proposed for diabetic wounds, but concerns about its delivery and cost have been raised [40, 41]. Therefore, understanding the regulation of VEGF-A is important for the appropriate control of wound healing. In the present study, the effect of Exo-shEGR1 on wound healing of mice was also determined, which was consistent with observations in cellular experiments, suggesting the implication of the lncRNA-SENCR/DKC1/VEGF-A axis in hADSC-Exo EGR-1-mediated wound healing.

Taken together, both in vitro and in vivo experiments supported the protective effect of hADSC-Exo EGR-1 in accelerating wound healing. Further mechanistic analysis

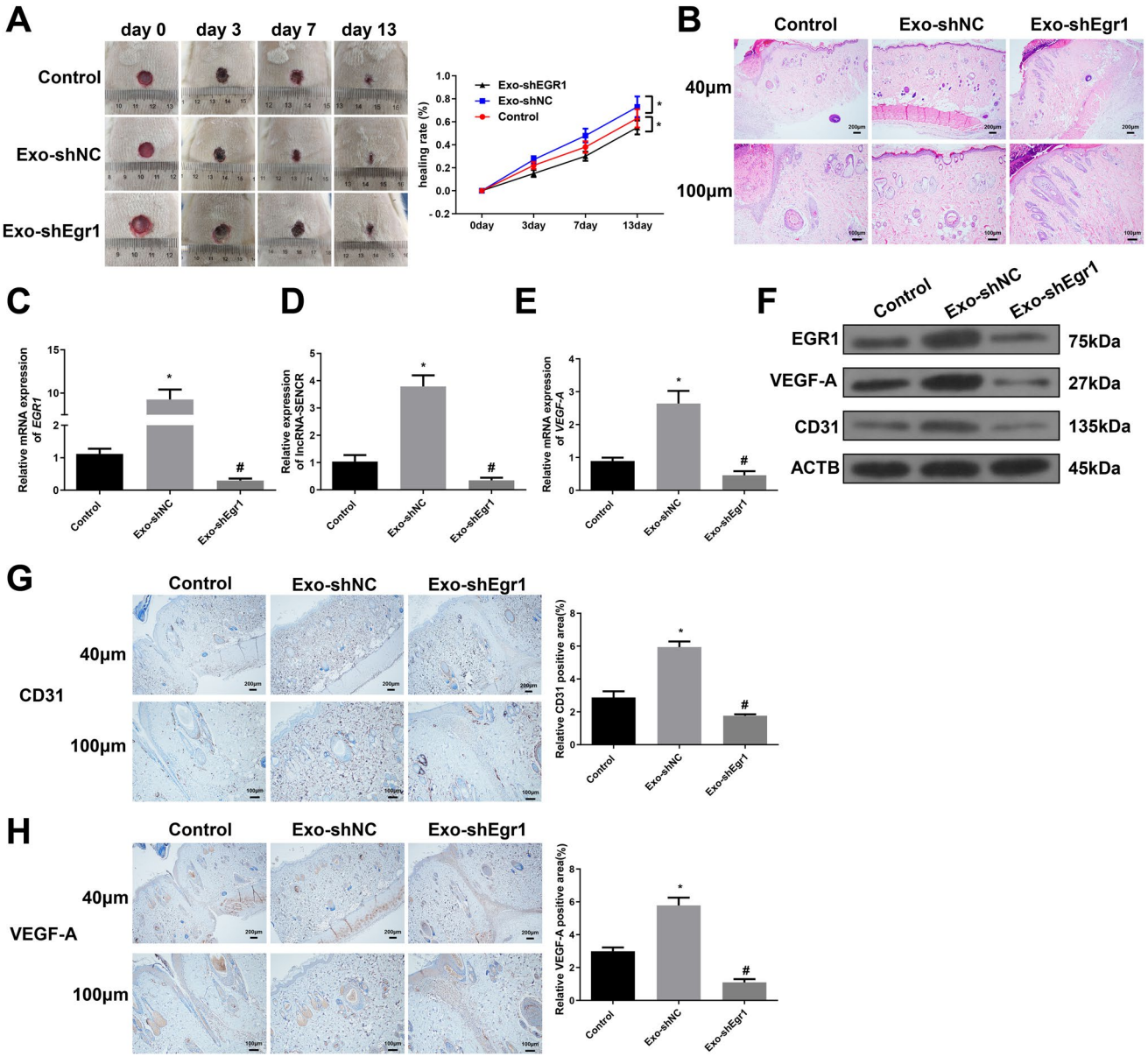

Fig. 6 Verifying the effect of Exo-shEGR1 in wound healing in mouse. **A** images of wound healing in mouse after Exo-shNC, Exo-shEGR1 or PBS treatment for 0, 3, 7, 13 days; **B** the effect of Exo-shNC, Exo-shEGR1 or PBS in mouse was assessed by H&E staining; **C** qPCR detected the expression of *EGR1* in mouse after Exo-shNC, Exo-shEGR1 or PBS treatment; **D** qPCR detected the expression of lncRNA-SENCR in mouse after Exo-shNC, Exo-shEGR1 or PBS treatment; **E** qPCR detected the expression of VEGF-A in mouse after Exo-shNC, Exo-shEGR1 or PBS treatment; **F** western blot measured the expressions of EGR1, VEGF-A and CD31 in mouse after Exo-shNC, Exo-shEGR1 or PBS treatment; **G** Immunohistochemistry was used to detect the effect of Exo-shNC, Exo-shEGR1 or PBS treatment on CD31; **H** Immunohistochemistry was used to detect the effect of Exo-shNC, Exo-shEGR1 or PBS treatment on VEGF-A, *Exo-shNC group compared with control group, $p < 0.05$; #, Exo-shEGR1 group compared with Exo-shNC group, $p < 0.05$. Each group had 6 mice and all experiments were conducted for three times

demonstrated that EGR-1 can interact with the lncRNA-SENCR promoter to activate the DKC1/VEGF-A signaling pathway, thus improving tissue repair and wound healing. Our study proposes a possible mechanism to better understand the role of hADSC-Exos in wound healing. As mentioned before, the biological function of EGR-1 may change with cellular content, and more experiments are, therefore, required to validate the role of hADSC-Exo EGR-1 in wound healing.

Supplementary Information The online version contains supplementary material available at https://doi.org/10.1007/s13577-022-00732-2.

Acknowledgements Not applicable.

Funding This study was supported by the General Program of Natural Science Foundation of Hunan Province (Grant No. 2021JJ30928).

Declarations

Conflict of interest The authors declare that they have no competing interests.

Ethical approval The experimental design involving human was approved by the ethical committee of the Second Xiangya Hospital (approval no. 2019224) and conformed to the Declaration of Helsinki. Human adipose tissues were collected after each enrolled patient provided written informed consent. Animal experiments complied with the regulations and codes of practice for the management of laboratory animals and were reviewed and approved by the ethical committee of the Second Xiangya Hospital (approval no. 2020256).

References

1. Hata Y, Iida O, Ito N, et al. Roles of angioplasty with drug-coated balloon for chronic ischemia in wound healing. J Endovasc Ther. 2021;28:778–87.
2. Veith AP, Henderson K, Spencer A, Sligar AD, Baker AB. Therapeutic strategies for enhancing angiogenesis in wound healing. Adv Drug Deliv Rev. 2019;146:97–125.
3. Xi Y, Ge J, Guo Y, Lei B, Ma PX. Biomimetic elastomeric polypeptide-based nanofibrous matrix for overcoming multidrug-resistant bacteria and enhancing full-thickness wound healing/skin regeneration. ACS Nano. 2018;12:10772–84.
4. Ullm F, Pompe T. Fibrillar biopolymer-based scaffolds to study macrophage-fibroblast crosstalk in wound repair. Biol Chem. 2021;402:1309–24.
5. Wilkinson HN, Hardman MJ. Wound healing: cellular mechanisms and pathological outcomes. Open Biol. 2020;10:200223.
6. Goodarzi P, Falahzadeh K, Nematizadeh M, et al. Tissue engineered skin substitutes. Adv Exp Med Biol. 2018;1107:143–88.
7. Okonkwo UA, DiPietro LA. Diabetes and wound angiogenesis. Int J Mol Sci. 2017;18:1419.
8. Wang J, Chen Y, Zeng Z, et al. HMGA2 contributes to vascular development and sprouting angiogenesis by promoting IGFBP2 production. Exp Cell Res. 2021;408: 112831.
9. Hassanshahi A, Hassanshahi M, Khabbazi S, et al. Adipose-derived stem cells for wound healing. J Cell Physiol. 2019;234:7903–14.
10. Gadelkarim M, Abushouk AI, Ghanem E, Hamaad AM, Saad AM, Abdel-Daim MM. Adipose-derived stem cells: effectiveness and advances in delivery in diabetic wound healing. Biomed Pharmacother. 2018;107:625–33.
11. Zhang L, Yu D. Exosomes in cancer development, metastasis, and immunity. Biochim Biophys Acta Rev Cancer. 2019;1871:455–68.
12. Kalluri R, LeBleu VS. The biology, function, and biomedical applications of exosomes. Science. 2020;367:eaau6977.
13. Han Y, Ren J, Bai Y, Pei X, Han Y. Exosomes from hypoxia-treated human adipose-derived mesenchymal stem cells enhance angiogenesis through VEGF/VEGF-R. Int J Biochem Cell Biol. 2019;109:59–68.
14. Qiu H, Liu S, Wu K, Zhao R, Cao L, Wang H. Prospective application of exosomes derived from adipose-derived stem cells in skin wound healing: a review. J Cosmet Dermatol. 2020;19:574–81.
15. Goodarzi P, Larijani B, Alavi-Moghadam S, et al. Mesenchymal stem cells-derived exosomes for wound regeneration. Adv Exp Med Biol. 2018;1119:119–31.
16. Zhao B, Zhang X, Zhang Y, et al. Human exosomes accelerate cutaneous wound healing by promoting collagen synthesis in a diabetic mouse model. Stem Cells Dev. 2021;30:922–33.
17. Davis FM, Kimball A, Boniakowski A, Gallagher K. Dysfunctional wound healing in diabetic foot ulcers: new crossroads. Curr Diab Rep. 2018;18:2.
18. Trinh NT, Yamashita T, Ohneda K, et al. Increased expression of EGR-1 in diabetic human adipose tissue-derived mesenchymal stem cells reduces their wound healing capacity. Stem Cells Dev. 2016;25:760–73.
19. Havis E, Duprez D. EGR1 transcription factor is a multifaceted regulator of matrix production in tendons and other connective tissues. Int J Mol Sci. 2020;21:1664.
20. Qian ZY, Jiang F, Tang J, et al. Potential roles of lncRNA-Cox2 and EGR1 in regulating epidural fibrosis following laminectomy. Eur Rev Med Pharmacol Sci. 2019;23:7191–9.
21. Gaut L, Robert N, Delalande A, Bonnin MA, Pichon C, Duprez D. EGR1 regulates transcription downstream of mechanical signals during tendon formation and healing. PLoS ONE. 2016;11:e0166237.
22. Guo B, Tian XC, Li DD, et al. Expression, regulation and function of Egr1 during implantation and decidualization in mice. Cell Cycle. 2014;13:2626–40.
23. Livak KJ, Schmittgen TD. Analysis of relative gene expression data using real-time quantitative PCR and the 2(-Delta Delta C(T)) Method. Methods. 2001;25:402–8.
24. Habibi M, Chehelcheraghi F. Effect of bone marrow mesenchymal stem cell sheets on skin capillary parameters in a diabetic wound model: a novel preliminary study. Iran Biomed J. 2021;25:334–42.
25. Parmar D, Apte M. Angiopoietin inhibitors: a review on targeting tumor angiogenesis. Eur J Pharmacol. 2021;899:174021.
26. Casado-Diaz A, Quesada-Gomez JM, Dorado G. Extracellular vesicles derived from mesenchymal stem cells (MSC) in regenerative medicine: applications in skin wound healing. Front Bioeng Biotechnol. 2020;8:146.
27. Lai RC, Yeo RW, Lim SK. Mesenchymal stem cell exosomes. Semin Cell Dev Biol. 2015;40:82–8.
28. Hu P, Yang Q, Wang Q, et al. Mesenchymal stromal cells-exosomes: a promising cell-free therapeutic tool for wound healing and cutaneous regeneration. Burns Trauma. 2019;7:38.
29. Tkach M, Thery C. Communication by extracellular vesicles: where we are and where we need to go. Cell. 2016;164:1226–32.
30. Li G, Chen Y, Han Y, Ma T, Han Y. Human antigen R promotes angiogenesis of endothelial cells cultured with adipose stem cells derived exosomes via overexpression of vascular endothelial growth factor in vitro. Adipocyte. 2021;10:475–82.
31. Kou X, Xu X, Chen C, et al. The Fas/Fap-1/Cav-1 complex regulates IL-1RA secretion in mesenchymal stem cells to accelerate wound healing. Sci Transl Med. 2018;10:eaai8524.
32. Huh JE, Nam DW, Baek YH, et al. Formononetin accelerates wound repair by the regulation of early growth response factor-1 transcription factor through the phosphorylation of the ERK and p38 MAPK pathways. Int Immunopharmacol. 2011;11:46–54.
33. Tkalcevic VI, Cuzic S, Brajsa K, et al. Enhancement by PL 14736 of granulation and collagen organization in healing wounds and the potential role of egr-1 expression. Eur J Pharmacol. 2007;570:212–21.
34. Bellodi C, Krasnykh O, Haynes N, et al. Loss of function of the tumor suppressor DKC1 perturbs p27 translation control and contributes to pituitary tumorigenesis. Cancer Res. 2010;70:6026–35.
35. O'Brien R, Tran SL, Maritz MF, et al. MYC-driven neuroblastomas are addicted to a telomerase-independent function of dyskerin. Cancer Res. 2016;76:3604–17.

36. Hou P, Shi P, Jiang T, et al. DKC1 enhances angiogenesis by promoting HIF-1alpha transcription and facilitates metastasis in colorectal cancer. Br J Cancer. 2020;122:668–79.
37. Zhu Y, Wang Y, Jia Y, Xu J, Chai Y. Roxadustat promotes angiogenesis through HIF-1alpha/VEGF/VEGFR2 signaling and accelerates cutaneous wound healing in diabetic rats. Wound Repair Regen. 2019;27:324–34.
38. Rattner A, Williams J, Nathans J. Roles of HIFs and VEGF in angiogenesis in the retina and brain. J Clin Invest. 2019;129:3807–20.
39. Melincovici CS, Bosca AB, Susman S, et al. Vascular endothelial growth factor (VEGF) - key factor in normal and pathological angiogenesis. Rom J Morphol Embryol. 2018;59:455–67.
40. Choi SM, Lee KM, Kim HJ, et al. Effects of structurally stabilized EGF and bFGF on wound healing in type I and type II diabetic mice. Acta Biomater. 2018;66:325–34.
41. Guc E, Briquez PS, Foretay D, et al. Local induction of lymphangiogenesis with engineered fibrin-binding VEGF-C promotes wound healing by increasing immune cell trafficking and matrix remodeling. Biomaterials. 2017;131:160–75.